UDC 005.922.52:004.932, DOI: 10.2298/CSIS1001063S

3D Mesh Skeleton Extraction Using Prominent Segmentation

Xiaopeng SUN[1], J. PAN[2], and Xiaopeng WEI[3]

[1] School of Mechanical & Engineering, Dalian University of Technology,
Dalian 116024, China
xpzhsun@gmail.com
[2] Department of Computer & Information Technology,
Liaoning Normal University, Dalian 116029, China
cadcg2008@gmail.com
[3] Key Laboratory of Advanced Design and Intelligent Computing (Dalian University),
Ministry of Education, Dalian 116622, China
xiaopengwei@gmail.com

Abstract. Skeleton of 3D mesh is a fundamental shape feature, and is useful for shape description and other many applications in 3D Digital Geometry Processing. This paper presents a novel skeleton extraction algorithm based on feature point and core extraction by the Multi-dimensional scaling (MDS) transformation. The algorithm first straights the folded prominent branch up, as well as the prominent shape feature points of mesh are computed, a meaningful segmentation is applied under the direction of feature points. The Node-ring of all segmented components is defined by discrete geodesic path on mesh surface, and then the skeleton of every segmented component is defined as the link of the Node-ring's center. As to the core component without prominent feature points, principal curve is used to fit its skeleton. Our algorithm is simple, and invariant both to the pose of the mesh and to the different proportions of model's components.

Keywords: Skeleton, MDS, Discrete geodesic path, Node-ring.

1. Introduction

In recent years, how to design a simple and robust algorithm to extract the skeleton of object with less memory cost and shape information loss has become a fundamental problem of information visualization and pattern recognition [1] et al.

Most existing algorithms were developed for 3D medical image analysis with volumetric data as input, and little work on the 3D mesh models, which are represented as a polygonal list. But because of the property of reducing the dimension of the problem, skeleton has shown its promising advantage in the application of geometry and topology description with its simplicity in region of 3D Digital Geometry Processing (DGP), such as deformation[2][3], shape recognition and retrieval[4][5], mesh editing[6], simplification[7], motion control and collision detection[8], segmentation[9] et al.

Meaningful mesh segmentation is another fundamental problem in DGP, which decompose 3D surface meshes into functional shape components, not only provides semantic information about the underlying mesh, but also could be used to guide several mesh processing algorithms, including skeleton extraction, modeling, morphing, shape-based 3D shape retrieval, and texture mapping[9] et al. All of these applications benefit from mesh meaningful segmentations that obey human intuition. Good 3D mesh segmentation will result in high quality skeleton.

In this paper, we introduce a novel skeleton extraction algorithm based on meaningful shape decomposition, which segment the 3D mesh under the direction of the prominent feature point and core. The challenge of this algorithm is that, the triangle patch size should be uniform in general level to keep a high precision, because the Node-ring is defined by the length of discrete geodesic path, or subdivision must be applied firstly. And to those meshes with 5,000 vertices or more, efficient memory management should be considered to improve computing speed of shortest path between all pair vertices of mesh, or simplification must be applied as a preprocessing. Due to the transformation of MDS and the direction of prominent feature points, we decompose the mesh into several prominent meaningful branch components and a core component, and then compute the skeleton of meaningful components respectively, so our algorithm is robust, simple, and pose-invariance.

2. Related works

Cornea et al. presented a comprehensive overview on curve-skeleton properties, applications and algorithms[1]. In recent decades, hundreds research works have been published in very extensive application regions.

The skeleton model is initially defined as a collection of the centre of the largest inscribed sphere[10], and is used extensively in virtual navigation, traditional computer graphics, medical image segmentation and quantification, registration, matching, 3D mesh morphing, segmentation, and analysis of scientific data et al.

And the various applications required their own desired properties of the skeleton; for example, the skeleton should be topologically equivalent to the original object in shape recognition, and must be invariant under isometric transformations[4][11]. In the application of shape compression and volume animation, the skeleton should provide enough information to reconstruct a 3D object completely from its medial skeleton representation by computing the union of maximal inscribed balls[12]. And the skeleton should be its centeredness within the 3D object[13]; the logical components of the object should have a one-to-one correspondence with the logical components of the skeleton[14][15]; be not very sensitive to little noise in the boundary;

approximate to the complex components of an object, and reflect the natural hierarchy of these complexities, et al.

Commonly, the curve-skeleton algorithms can be divided into three classes: topological thinning (grassfire propagation), distance transform based (ridge detection) and Voronoi diagram based[16][17]. More recently in 2007, Cornea et al. initially categorize the algorithms into four new classes: thinning and boundary propagation, using a distance field, geometric methods, general field functions[1]. Our algorithm is a geometric method.

The basic idea of the thinning algorithm to extract the skeleton of voxel model is: from outside to inside, layer upon layer strips[18]. To judge one voxel whether needed to be stripped off is comparatively time-consuming work, therefore, G. Bertrand proposes a parallel thinning algorithm[19]. However, many problems are still not solved well at present, such as some skeletons are not continuous and affected by noise, often contain some invalid branches. And skeleton with a higher topology and centrality is very hard to extract et al.

Skeleton extraction based on the distance transformation algorithm can ensure the centrality of skeleton points, but is weak in keeping original topology. The algorithm based on the Level Set[20] has a better stability and higher topology independency, can effectively overcome cusp and skeleton fracture, but even Fast Marching Method is used, its computational complexity is still very high. A snake model could adjust skeleton position, to improve skeleton’s centricity, but increased complexity as well.

Compared with the distance transform and thinning algorithms, the algorithm based on shape classification or segmentation has a more remarkable superiority [21][22]. Based on the topological connection information, segmentation is applied firstly; then the skeleton is extracted from the segmentation results, to reduce the complexity and enhance skeleton's precision.

On the other hand, the 3D skeleton can be used to guide segmentation in turn, to get a more meaningful segmentation and obey the Minimal Rule better[9][23]. Most skeleton extraction works involved with segmentation are sensitive to the pose of the model. For instance, very different segmentations will be produced when the models of human have their arms folded or not, due to the vital difference of curvature (or dihedral angles). By decomposing a 3D model into approximate convex components, Lien etc calculated the vertices convexity-concavity firstly, and then extracted the skeleton by iteration, but the obtained skeleton had a worse centricity, and hard to establish the level relations[24].

Segmentation is a classical problem in processing of 3D mesh surfaces, and other types of multimedia data, and most of these methods have been evaluated only by visual inspection of results, reference [23] provide four quantitative metrics for evaluation of mesh segmentation algorithms, that are cut discrepancy, Hamming distance, rand index, and consistency error. The focus of the segmentation in this paper is to find the prominent branch and improve the speed, so we neglect the above four quantitative metrics, and leave the jaggy boundaries to the feature.

3. Overview

Inspired by the work of Sagi Katz etc [25], we proposed a novel skeleton extract algorithm, which based on segmentation of prominent branches and geodesic path.

Given an 3D mesh *S* in Euclid space, its vertices set is $\{v_i|1\leq i\leq n\}$, and $\delta_{ij}=GeoDist(v_i,v_j)$ is defined as the weighted discrete geodesic distance between every two adjacent vertex (v_i,v_j) on *S* [14]. Based on Fast Marching method in [26], to every pair of vertices (v_i,v_j) on *S*, the discrete geodesic distance $\delta_{ij}=GeoDist(v_i,v_j)$ and the shortest path $ShortPath(v_i,v_j)$ can be obtained.

Our algorithm has the following steps:

Based on the theory of multi-dimensional scaling (MDS), the mesh *S* is transformed from Euclid space into its pose-invariant representation S_{MDS} in MDS space, and the folded organs branches are prominently straightened.

Robust prominent feature points PF_i, $i=1,2,\dots,k$ can be located on the convex-hull in MDS space, and then *S* is segmented into several prominent meaningful branch components $S_1, S_2,\dots S_k$ and a core component S_0.

Define the points located on the boundary between the components as **connecting ring** $LOOP_i$.

Compute the discrete geodesic path from PF_i to every point on $LOOP_i$, the space structure of there shortest paths can be represented by a tree with its root on the feature point.

From the root PF_i to the $LOOP_i$, we define 20-30 level sets of mesh points, called **node ring**.

Fitting the connect line of the center of node ring with KS principal curve, skeletons of branches are computed. And the skeleton of core is computed specially.

Finally, joint the branch skeleton of every component together in a simple way, the single connected skeleton of *S* obtained.

Every sub-mesh's node ring is defined by the discrete geodesic distance on mesh surface, and the skeleton of each sub-mesh is extracted, our algorithm can deal with bending posture and overcome of noise, and is simple, robust, and pose-invariant.

4. Segmentation of prominent brances

Due to noise, it is difficult to extract feature points on mesh model *S* directly. The MDS (Multi-dimensional scaling) is used to transform *S* into the mesh S_{MDS} in MDS space, and let d_{ij} be the Euclidean distance between the corresponding points of (v_i,v_j) on S_{MDS}, and then the distances matrix is obtained.

After 30-50 iteration optimizations by the stress function in [25], the topology information of model *S* is kept, but the position of every vertex is changed, every folded prominent components of a model are straightened, we denoted the optimization process by $S \rightarrow S_{MDS}$.

Based on MDS transformation, $S \rightarrow S_{MDS}$ can filter the noise on model S globally, and obtained a new mesh S_{MDS} with every folded prominent branch straightened. We extract the prominent feature points on S_{MDS} to overcome the interference of noise.

In other words, if a vertex be a prominent feature point on S, it should reside on a tip of S_{MDS}, (i.e. on the convex-hull of S_{MDS}), and it is a local maximum of the sum of the geodesic distance to any other vertex[25].

We denote the k prominent feature points on S_{MDS} by PF_i, $i=1,2,\ldots,k$ (e.g. the red points in Fig. 1)

Fig. 1. Feature points (in red).

Then we define a mirror sphere on S_{MDS}, so every vertex v of S_{MDS} has a image v_{mirror} outside the mirror sphere[25]. Define the core of mesh S_{MDS} as a set of the vertices reside on the convex-hull, and denoted it by SC_{MDS}. Obviously, the prominent branches and feature points of S_{MDS} become the internal of the convex-hull.

Let the number of feature points PF_i on S_{MDS} be k, so its corresponding prominent branches number is k too. After the mirror transformation, the prominent branches will be cut by the core component extraction, then we obtain $k+1$ meaningful segmentation components $S_0, S_1, S_2, \ldots S_k$ of mesh S, where S_0 is the core component corresponding to SC_{MDS} (e.g. the green component in Fig. 2-(e)), and S_i, $i=1,2,\ldots,k$ is sub-mesh composed of k prominent branches (e.g. the white, pink, red and yellow components in Fig. 2-(e)).

(a)source mesh (b)mesh (c)Spherical mirroring (d)core (e)segmentation.

Fig. 2. Spherical mirroring segmentation

5. Construction of shortest path and skeleton

5.1. Connecting ring

Let S_0, S_1, S_2,…S_k be the $k+1$ segmentation of model S, and denoted the vertex set on the common boundary between sub-mesh S_i, $i=1,2,\ldots,k$ and S_0 by $LOOP_i=\delta S_0 \cap \delta S_i$, (e.g. the red points in Fig. 3-(a)), then named this vertex set as a **connecting ring** between every sub-mesh S_i and the core component S_0.

For every shortest path between prominent feature point PF_i and the vertex in the corresponding connecting link $LOOP_i$, obviously the number of such shortest path is more than one, and the space structure of these shortest paths can be represented by a tree whose root is the feature point PF_i, we denote this tree as $Tree_i$.

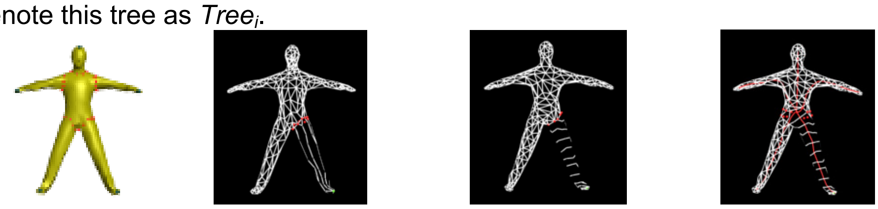

(a)Connecting Ring (b) shortest path (c) Node ring (d) Skeleton

Fig. 3. Connecting Ring and skeleton of branch

5.2. Node ring of S_i and skeleton computing

For the shortest path tree $Tree_i$ with the feature point PF_i as root in the sub-mesh S_i, the depth from the root node PF_i to each leaf node on corresponding connecting ring $LOOP_i$ is different, and corresponding discrete geodesic distances is different too.

The shortest path set of feature point PF_i on sub-mesh S_i to any v_j on $LOOP_i$ is denoted by $ShortPath(PF_i,v_j)$ (e.g. Fig. 3-(b)), the geodesic length of corresponding shortest path is denoted by $sp(v_j)=\|ShortPath(PF_i,v_j)\|$, and the maximum and the minimum length of all the discrete geodesic distance on this set are denoted by $sp_{max}=\max\{\|ShortPath(PF_i,v_j)\|\}$ and $sp_{min}=\min\{\|ShortPath(PF_i,v_j)\|\}$ respectively.

Let $\varDelta sp= sp_{max}/m$, $\delta sp= sp_{min}/m$, then define the m **node rings** (e.g. the level ring within the right leg in Fig. 3-(c)) of sub-mesh S_i as its m subsets of vertex set $H(v)=\cup\{v\in S_i|\delta sp\cdot t \le sp(v_j) \le \varDelta sp\cdot t\}$, where m is a nonnegative constant integer, let $t=1,2,\ldots, m$, and $C=\|H_t(v)\|$, then the center coordinates of node ring $H_t(v)$ be defined as:

$$Center\left(H_t\left(v\right)\right)=\sum_{c=1}^{C}\frac{Coordinate\left(H_t\left(v\right)\right)}{C}$$

Connect the centroid $Center(H_t(v))$ of successive level sets on sub-mesh S_i, and the center of $LOOP_i$, then the skeleton curve of sub-mesh S_i be constructed by the connected $m+1$ points (e.g. the red line within the right leg in Fig. 3-(d)).

Do the same processing to all sub-mesh $S_1, S_2, \ldots S_k$, we will get the skeleton of each prominent branch except S_0,which corresponds with the core component.

5.3. Skeleton of core components S_0

Due to the core component S_0 has no feature points, so a special consideration is needed to extract its skeleton.

For the core component S_0 with its gravity center located in internal, the KS principal curve algorithm in [27] is used to fit k lines which connected the central point of $LOOP_i$ and the center of core component S_0, the new skeleton S_0^{ks} is represented by principal curve. Connect the central point of $LOOP_i$ and relative nearer endpoint of S_0^{ks} by turn, the complete skeleton of model S is obtained.

For the core component S_0 with gravity center located in exterior, its skeleton could be obtained by following method：

For given S and its vertex set $\{v_i | 1 \le i \le n\}$ with coordinate set $\{x_i, y_i, z_i\}^n_{i=1}$, the moment (p, q, r)-*th* of discrete definition can be approximated by

$$m_{pqr}=\frac{1}{n}\sum_{i=1}^{n}x_i^p y_i^q z_i^r$$

According to its definition, the set of moments $\{m_{pqr}\}$ are uniquely, and are uniquely determined by the object, the first moments and second moments respectively represent the mesh's center of the mass and the three PCA axles [28]. Then, based on the first moment and second moment of the core component S_0, the gravity center, the PCA axles and three axis planes of core component S_0 can be obtained.

Let O be the gravity center of S_0, and sort the three main axles according to the axial length in descending order as A, B, C , let the base plane be OBC where the two shorter axis lie in , a constant h_0 is suitably chosen along OA, i.e. the longest axis direction. Horizontally cut the vertex set S_0 into m subsets with thickness h_0, denote the vertex subsets of S_0 by $H^0_t(v)$, $t=1,2,\ldots,m$, named $H^0_t(v)$ by the **central ring** of the core component S_0,with the central coordinate as

$$Center\left(H_t^0(v)\right)=\sum_{c=1}^{C^0}\frac{Coordinate\left(H_t^0(v)\right)}{C^0}$$

Where $C^0=\|H^0_t(v)\|$. Connect $Center(H^0_t(v))$ sequentially; the skeletal curve of core component S_0 will be a ks principal curve fitting of the lines by the *m* connecting points.

Our algorithm requests core component has the better convexity, then $Center(H^0_t(v))$ should locate within the projecting polygon of the vertex subset $H^0_t(v)$ on base plane *OBC*, otherwise, the skeleton will go out the core component S_0, and be not located in the internal of model *S* completely, this algorithm expiration.

6. Results and discussion

We use the Shape Benchmark database at Princeton university (Fig. 4-(h) exceptions) to test our algorithm. All data are recorded on an 2.20GHz Intel Core(TM) 2 Duo CPU E4500 machine with 2GB RAM and 128M GM, using a single thread implementation.

Table 1 shows the running time of computing the prominent feature point and skeleton for various 3D models.

Table 1. Computing time

Model	Vertices	Faces	Feature Points	Time(s)
M0235	408	812	5	0.311
M0336	1,557	3,110	6	3.813
M0324	1,564	3,124	6	4.001
M0031	1,802	3,548	5	4.876
M0178	914	1,824	5	1.871
M0071	420	836	6	0.345
M0095	956	1,908	6	2.062
M0000	3,117	6,250	9	14.794
M0050	1,455	2,906	3	3.304
M0058	477	950	5	0.502
M0104	906	1,808	7	1.831

In Fig. 4, the green dots are the prominent feature points, yellow points are two endpoints of the core component skeleton, and red lines are the skeletons of its core and branches.

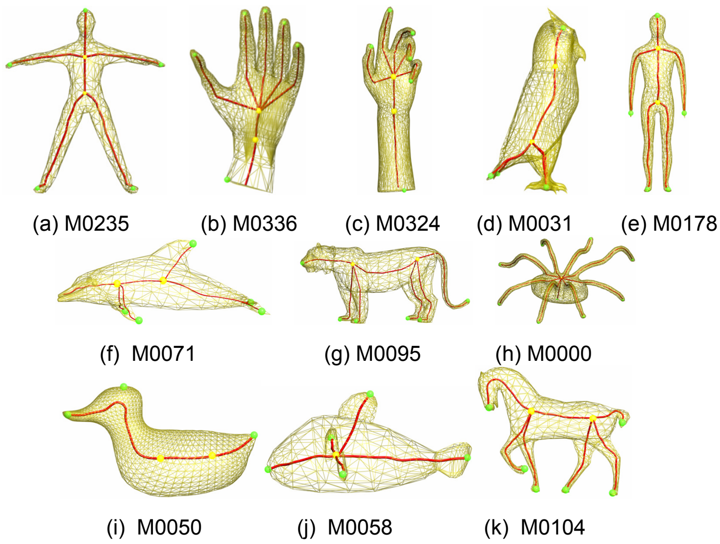

Fig. 4. Skeletons of some models

Although the optimization process $S \to S_{MDS}$ stretching the mesh S, to help the extraction of prominent feature points on the pose-invariant model S_{MDS}, can overcome the interference of noise, but on the other hand, some slight partial characteristic be shielded, as shown by owl's beak in Fig. 4-(d), and ears in Fig. 4-(g) and Fig. 4-(k) etc, where the smaller feature points are shielded by the more prominent neighboring extreme points. In addition, to those models without prominent branches, the obtained skeleton does not have clear meaning, just as Fig. 4-(h) ellipsoid part shows.

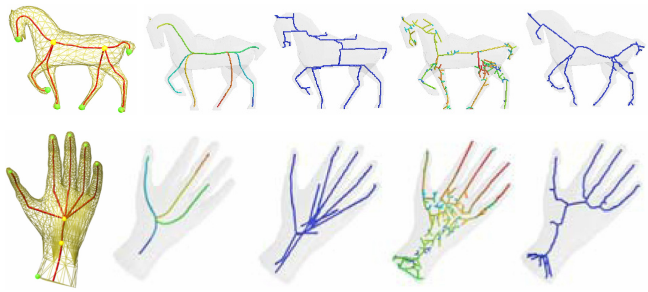

(a)ours (b)potential field (c)geometric (d)distance field (e)thinning

Fig. 5. Skeleton obtained using different algorithms

The skeleton of the prominent branch start not from the feature point PF_i, but from the centroids $Center(H_t(v))$ of successive level sets of S_i, until arrive the center of $LOOP_i$, as Fig. 4-(b) and Fig. 4-(c) shows, skeleton starts away from the green feature points at the bottom of the wrist; and as a fact, the green feature point and the prominent branch skeleton's red endpoint are also separate in other results.

Fig. 5 shows the results of our algorithm and the algorithm of thinning distance field, geometric, potential field method. The left column is produced by our algorithm, and other four columns are provided by [1]. Obviously, the comparison shows that our algorithm is more effective than others.

Let N be the number of faces in the original model S, then the computational complexity of MDS is bounded by $O(N^2)$; the prominent feature point extraction takes $O(N\log N)$; the $k+1$ segmentation costs $O(N\log N)$; connecting ring, node ring and center ring costs $O(\log N+N)$; skeleton fitting costs $O(N)$; thus the overall time complexity is $O(N^2+N\log N+N+\log N)=O(N^2)$.

In addition, our algorithm can extract the skeleton of simply connected and complex topology 3D model with its genus<1. For constructing by connecting prominent feature points PF_i and the points on connecting ring $LOOP_i$, the pyramidal shortest path set guarantees the skeleton to locate in the internal of sub-mesh S_i, and enhances the centricity of skeleton.

7. Conclusion and feature work

We proposed a novel algorithm for 3D mesh skeleton extraction. The advantage of this approach is that: Our algorithm does not involve complicated mathematical tools. Compared with snake and level set[20], our algorithm has a lower complexity. It obtains the prominent feature points by the preprocessing of MDS transformation, and then extracts the local skeleton under the guidance of the prominent feature points and the strategy of segmentation, reduces the influence of noise, and improves the efficiency. The skeleton obtained is topology-invariant and pose-invariant. The shortest path's search is carried on the sub-mesh, overcomes the difficulty to judge branches and select feature points; our algorithm requires neither prior-knowledge of the number of feature points nor any interactive user parameters; and our skeleton is invariant to the pose of the mesh model.

The limitations of our algorithm are: When the core component has prominent concavity, its gravity center located outside the projection of core component on base plane OBC, skeleton will go out the surface. In addition, we connected the skeleton of core component and that of other prominent branches without trimming strategy, then the skeleton was not guaranteed to be smoothing in any case. And obviously, the prominent feature points of sub-mesh S_i used as the root of shortest path tree can be used to roughly determine skeleton line shape and trends on the consideration of its relative position to connecting ring, this potential information was not fully used for now.

8. Acknowledgment

This work is supported in part by National Natural Science Foundation of China with projects No. 60873110, No. 60875046, and No. 60533090.

9. References

1. Cornea, N. D., Min, P.: Curve-skeleton properties, applications, and algorithms. IEEE Transactions on Visualization and Computer Graphics, vol. 13, No. 3, 530–548. (2007)
2. Oscar Kin-Chung Au, Chiew-Lan Tai, Hung-Kuo Chu, Daniel Cohen-Or, Tong-Yee Lee: Skeleton Extraction by Mesh Contraction. ACM Transactions on Graphics (SIGGRAPH 2008 issue), Vol. 27, No. 3, 44:1-44:10. (2008)
3. Han-Bing Yan, Shi-Min Hu, Ralph R Martin, and Yong-Liang Yang: Shape Deformation using a Skeleton to Drive Simplex Transformations. IEEE Transaction on Visualization and Computer Graphics, vol. 14, No. 3, 693-706. (2008)
4. Masaki Hilaga,Yoshihisa Shinagawa,Taku Kohmura, Tosiyasu L.Kunii: Topology Matching for Fully Automatic Similarity Estimation of 3D Shapes. In Proceedings of ACM SIGGRAPH. Los Angeles, USA, 203-212. (2001)
5. Sundar, H., Silver, D., Gagvani, N., Dickinson S.: Skeleton based shape matching and retrieval. In Proceedings of International Conference on Shape Modeling and Applications, Seoul, Korea,130-139. (2003)
6. Tao Ju, Qian-Yi Zhou, Shi-Min Hu: Editing The Topology of 3D Models by Sketching. ACM SIGGRAPH 2007, ACM Transactions on Graphics, vol. 26, No. 3, 42:1-42:10. (2007)
7. Tam, R., Heidrich W.: Shape simplifications based on the medial axis transform. In Proceedings of the 14th IEEE Visualization, Seattle, WA, USA, 63-70. (2003)
8. Jianfei Liu, Xiaopeng Zhang, Qingqiong Deng: Structural Volume Skeletonization and Visibility Computation for Virtual Endoscope. Journal of Computer-Aided Design & Computer Graphics, vol. 19, 1352-1358. (2007)
9. Xiaopeng Sun, Hua Li: A Survey of 3D Mesh Model Segmentation and Application. Journal of Computer-Aided Design & Computer Graphics, vol. 17, No. 8, 1647-1655. (2005)
10. Blum H.: A Transformation for Extracting New Descriptors of Models for the Perception of Speech and Visual Form. W. Walthen-Dunn, ed., US: MIT Press, Combridge. (1967)
11. Cornea N.D., Demirci M.F., Silver D., Shokoufandeh A., Dickinson S. J., Kantor P. B.: 3D Object Retrieval using Many-to-many Matching of Curve Skeletons, In Proceedings of Shape Modeling and Applications, Cambridge, MA, USA. (2005)
12. Gagvani, N.,Silver D.: Animating volumetric models. Academic Press Professional, vol. 63, No. 6, 443-458. (2001)
13. Dey, T.K., Sun J.: Defining and Computing Curve-Skeletons with Medial Geodesic Function, In Proceedings of Eurographics Symp. Geometry Processing, Cagliari, Sardinia, Italy,143-152.(2006)
14. Sagi Katz, Ayellet Tal: Hierarchical Mesh Decomposition using Fuzzy Clustering and Cuts. ACM Transactions on Graphics, vol. 22, No. 3, 954-961. (2003)
15. Robert A., Katz, Stephen M., Pizer: Untangling the Blum Medial Axis Transform. International Journal of Computer Vision, vol. 55, No. 2-3, 139-153. (2003)

16. Ma, W., Wu, F., Ouhyoung M.: Skeleton Extraction of 3D Objects with Radial Basis Functions. IEEE Proceedings of Shape Modeling International. Seoul, Korea, 207-215. (2003)
17. Telea, A., Vilanova A.: A robust level-set algorithm for centerline extraction, in Eurographics/IEEE Symposium on Visualization, Grenoble, France , 185–194. (2003)
18. Zhang, X., Liu, J., Jaeger Z. Li. M.: Volume decomposition and hierarchical skeletonization. In VRCAI '08: Proceedings of The 7th ACM International Conference on Virtual-Reality Continuum and Its Applications in Industry. Singapore; December. (2008)
19. Bertrand, G.: A parallel thinning algorithm for medial surfaces. Pattern Recognition Letters, vol. 16, No. 9, 979-986.(1995)
20. Osher, S., Sethian J.: Fronts propagating with curvature dependent speed: algorithm based on the Hamilton-Jacobi formulation, Journal of Computational Physics, vol 79, 1, 12-49. (1988)
21. Hoffman, D.D., Richards, W.A.: Parts of recognition. Cognition, vol. 18, 65-96. (1985)
22. Rom, H., Medioni, G.: Hierarchical decomposition and axial shape description. IEEE Transactions on Pattern Analysis and Machine Intelligence, vol. 15, No. 10, 973-981. (1993)
23. Xiaobai Chen, Aleksey Golovinskiy, Thomas Funkhouser A.: A benchmark for 3D mesh segmentation. ACM Trans. Graph. Vol. 28, No. 3. (2009)
24. Lien, J. M., Keyser, J., Amato, N. M.: Simultaneous shape decomposition and skeletonization. In Proceedings of the 2006 ACM symposium on Solid and physical modeling, Cardiff, Wales, UK, 219-228. (2006)
25. Sagi Katz, George Leifman, Ayellet Tal: Mesh segmentation using feature point and core extraction, The Visual Computer, vol. 21, No. 8/10, 649-658. (2005)
26. Vitaly Surazhsky, Tatiana Surazhsky, Danil Kirsanov, Steven J. Gorther, Hugues Hoppe: Fast Exact and Approximate Geodesics on Meshes. ACM Trans. on Graphics, vol. 24, No. 3, 553-560. (2005)
27. Verbeek, J. J., N,Kr se B Vlassis: A soft K-segments algorithm for principal curves. In: Proceedings of International Conference on Artificial Neural Networks, Vienna, 450-456. (2001)
28. Michael Elad, Ayellet, Sigal Ar: Content Based Retrieval of VRML Objects-An Iterative and Interactive Approach. In: Proceedings of the sixth Eurographics Workshop on Multimedia, Manchester UK, 107-118.(2001)

Xiaopeng Sun was born in P. R. China and received a PhD in Computer Science from Institute of Computing Technology, Chinese Academy of Sciences. He is a distinguished professor of LNNU, and his research interests include graphics and VR.

Xiaopeng Wei was born in P. R. China and received a PhD in Mechanical Engineering from Dalian University of Technology. He is a professor at DLUT, and his research interests include graphics.

Received: April 29, 2009; Accepted: October 03, 2009.